Functional gradient effects on the energy absorption of spider orb webs

Yang Guo, Zheng Chang, Bo Li, Zi-Long Zhao, Hong-Ping Zhao, Xi-Qiao Feng, and Huajian Gao

Citation: Appl. Phys. Lett. **113**, 103701 (2018); doi: 10.1063/1.5039710
View online: https://doi.org/10.1063/1.5039710
View Table of Contents: http://aip.scitation.org/toc/apl/113/10
Published by the American Institute of Physics

Functional gradient effects on the energy absorption of spider orb webs

Yang Guo,[1] Zheng Chang,[2] Bo Li,[1] Zi-Long Zhao,[3] Hong-Ping Zhao,[1,a)] Xi-Qiao Feng,[1,a)] and Huajian Gao[4,a)]
[1]*Department of Engineering Mechanics, Institute of Biomechanics and Medical Engineering, Tsinghua University, Beijing 100084, China*
[2]*College of Science, China Agricultural University, Beijing 100083, China*
[3]*Centre for Innovative Structures and Materials, School of Engineering, RMIT University, Melbourne 3001, Australia*
[4]*School of Engineering, Brown University, Providence, Rhode Island 02912, USA*

(Received 10 May 2018; accepted 16 July 2018; published online 4 September 2018)

Owing to their exquisite geometric structures and excellent mechanical properties, spider orb webs possess an outstanding ability to capture flying prey. In this work, we report a mechanism that enhances the energy absorption ability of spider webs. Through systematic measurements of the mechanical properties of both spiral and radial silks, we find that the spiral silks feature a distinct gradient variation in the diameter and tensile stiffness along the radial direction of the web, while the radial silks have a much higher but approximately uniform stiffness. A mechanical model is proposed to reveal the functional gradient effects on the energy absorption of the web. The results show that due to the gradient variation in the mechanical properties of spiral silks, the web exhibits a nearly uniform energy absorption ability regardless of the position where a flying prey impacts the web. This optimal structural feature of the web greatly enhances its efficiency and robustness in prey capture. This work not only helps understand the optimal mechanisms of spider webs but also provides clues for designing anti-impact structures. *Published by AIP Publishing.*
https://doi.org/10.1063/1.5039710

Through natural evolution, almost all biological materials possess exquisite structures adaptive to their essential functions, e.g., honeycombs,[1] silkworm cocoons,[2] seashells,[3] sponge endoskeletons,[4] and bovine horns.[5] For example, spider orb webs possess an ideal embodiment of lightweight network structures with superior strength and elasticity[6] to undertake various loads in the natural environment, e.g., the impacts of flying insects,[7–9] wind,[10] and water droplets.[11] The synergy between the mechanical properties and geometric structures of a spider web plays a significant role in its biological functions.[7,12,13]

Spiders have evolved a superior ability to adapt to the complex environment by architecting webs with different types of silks.[14,15] Strikingly, a spider can produce quite a few types of silk threads (e.g., major ampullate, minor ampullate, and flagelliform) with greatly different mechanical properties and geometric sizes in a web.[16,17] For example, radial silks usually have high stiffness, while spiral silks are soft and stretchable.[6] Silk threads produced by the same silk glands under different conditions can also exhibit varied mechanical properties.[18] In addition, the geometric features of a spider web, e.g., the angles and distances between adjacent threads[14,19] and the bizarre web decorations,[20] also affect its performance in prey capture. Owing to the optimal material properties and geometric structures, a spider web can not only sense and discern tiny vibrations induced by small preys[21] or wind[22] but also withstand the impacts of relatively large insects and birds.[7,9,23]

In spite of their different functions, the synergy of radial and spiral silks is crucial in the energy absorption and structural integrity of a spider web.[7,24] Owing to the balance between the mechanical properties of spiral silks and glue droplets, a web exhibits an outstanding energy absorption capacity and mechanical integrity.[25] Although the mechanical properties of spiral and radial silks have been studied separately,[6,17,26] it remains unclear how they are harmonized to enhance energy absorption ability.

In this work, we further investigate, both experimentally and theoretically, the energy absorption mechanisms of spider orb webs. Our experiments show that the mechanical properties of the spiral silks feature a significant gradient variation along the radial direction of a web. By using a mechanical model, we demonstrate an enhancing mechanism in spider webs, that is, the functional gradient properties endow the web with an optimal anti-impact performance no matter where an impact load is exerted.

Spiders *Araneus ventricosus* were raised in our laboratory. A wooden frame was used for each spider to weave a web. Once a web had been completely weaved, it was taken away from the wooden frame for further testing. To prevent rupture or stretch of any silks in this process, we used a metallic ring coated with a layer of double-sided tape[27] to fix the web [Fig. 1(a)]. The samples were manipulated under a microscope (VK-X100 K, Keyence, Japan). Before the mechanical measurement, each spiral silk sample was transferred from the web to a cardboard with a hole of diameter 5.5 mm. The two ends of the silk sample were fixed over the hole by double-sided tape. The spiral silk threads in a sector region of the web[28] were numbered along the radial direction, as shown in Fig. 1(a). The spiral silk threads in the outer circles were sufficiently long such that we could acquire several samples simultaneously using a cardboard with periodic holes.

[a)]Authors to whom correspondence should be addressed: zhaohp@tsinghua.edu.cn; fengxq@tsinghua.edu.cn; and huajian_gao@brown.edu

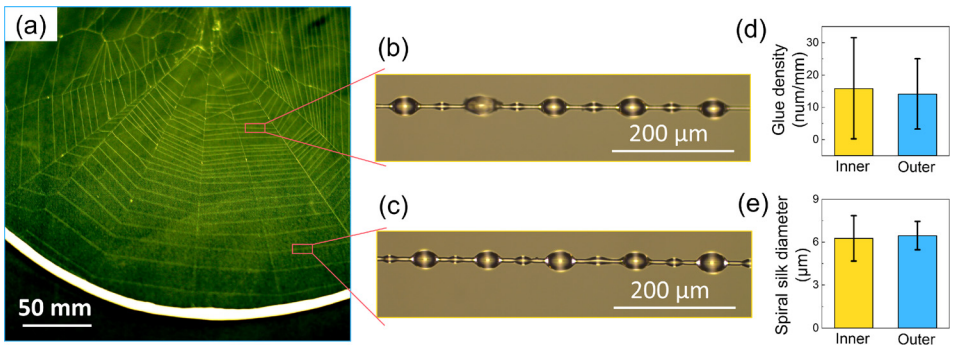

FIG. 1. Photos of (a) an orb web and its spiral silks covered with glue droplets in (b) the inner and (c) outer parts of the web, respectively. (d) Number densities of glue droplets and (e) diameters of spiral silks in the inner and outer parts of the web.

After the spiral silk threads had been removed, the radial silk samples were taken from the same web to set up the mechanical test.

A polarized optical microscope (VK-X100 K, Keyence, Japan) was used to observe and measure the morphology of the silks. The diameter of each spiral and radial silk was measured at least 5 times.[29] The average diameter of each sample would be used in the calculation of tensile stresses in its uniaxial tension test. The geometric parameters and number density of the glue droplets on the spiral silks were also measured.

Uniaxial tension tests were performed to determine the mechanical properties of the spiral and radial silk threads. A nanomechanical tensile testing machine (T150 UTM, Agilent, USA) with a load resolution of 50 nN and an extension resolution of 35 nm was used. A cardboard was used to fix the two ends of a silk sample. It was clamped by the grips of the testing machine and then cut through before loading such that only the silk sample sustained the tensile force. The tests were conducted at a fixed strain rate of 0.005/s at a room temperature of ~25 °C.

Finite element simulations are performed by using ABAQUS (6.10)[30,31] to investigate the energy absorption mechanisms of spider webs. In the simulations, we consider a two-dimensional orb web model, as shown in Fig. 2(a), which consists of 10 radial threads of 30 cm in diameter and 10 spiral threads. The radial silks are uniformly distributed, with an angle of 36° between any two neighboring silks, whereas the spiral silks have a uniform spacing of 15 mm. Since all threads are approximately in a uniaxial tensile stress state,[23,32] we used truss elements to mesh the web.[30,31,33] For simplicity, we assume that both radial and spiral silks are linear elastic,[12,34] while noting that our finite element simulations show that the nonlinear elasticity of the silks does not affect the main conclusions of this paper.

Displacement boundary conditions are specified at the outer ends of the radial silks. All outermost nodes of the web are fixed.[12,13] Small pre-stretches are applied to both the radial and spiral silks to mimic the prestress state in real orb webs.[12] In the model, a flying insect is assumed to impact at the middle position of the spiral silk, inducing a concentrated force F of 50 μN perpendicular to the web plane, as shown in Fig. 2. We perform numerical simulations to compare the stress and displacement distributions, as well as the energy absorption, when the force is exerted at different silks.

The morphology of spiral silks is shown in Figs. 1(b) and 1(c). In contrast to the smooth and non-sticky radial silk threads, the spiral silk threads are coated with a thin layer of sticky glue. As a consequence of Rayleigh instability, the coating glue typically breaks into uniformly distributed droplets, rendering a unique bead–chain appearance.[35] In each spiral silk thread, the glue droplets were equally distributed. The average number density of the droplets per unit length is about 15 mm^{-1} [Fig. 1(d)]. Our measurements showed that the diameters of the spiral silk threads in each web are close to each other, and their average diameter is 6.4±1.3 μm, as shown in Fig. 1(e).

Figures 3(a) and 3(b) show the experimental stress–strain curves of the spiral and radial silks, respectively. The spiral silks in each group (I, II, or III) were taken from the same sector of a web, as indicated by the inset in Fig. 3(a). It is seen that the mechanical properties of the spiral silk samples from the same thread are close to each other but exhibit a significant change along the radial direction of the web.

Figure 4 shows the gradient variations in the mechanical properties of spiral silk threads along the radial direction of

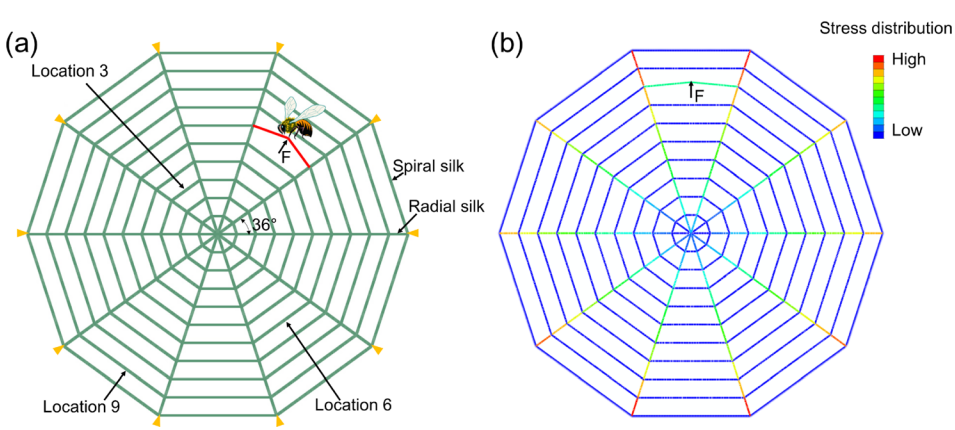

FIG. 2. (a) Calculation model for an orb web subjected to the normal impact of a prey and (b) stress distribution in the web when the prey impacts at the middle position of the 8th spiral silk.

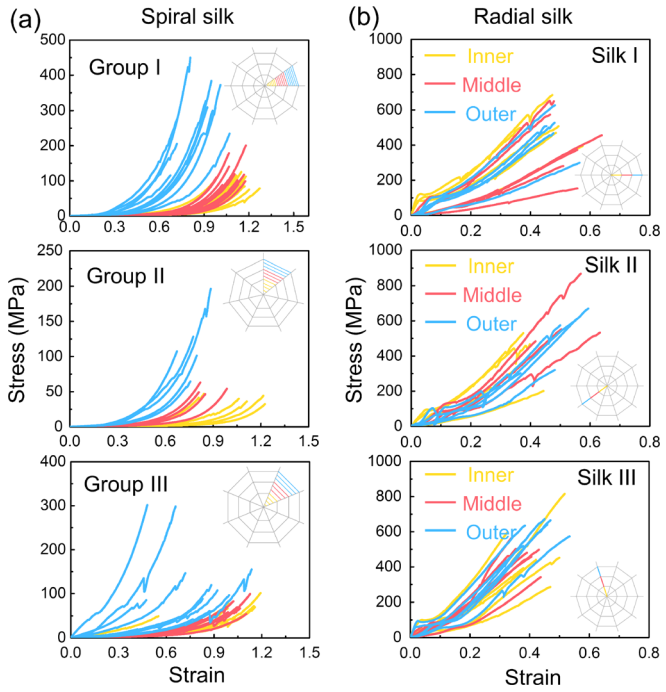

FIG. 3. Stress–strain curves of (a) spiral silks and (b) radial silks. The yellow, red, and blue curves correspond to silks in the inner, middle, and outer regions in the web, as shown in the insets.

the web. Three representative webs are given as examples. The spiral silks in the inner region of the web have a smaller stiffness (Young's modulus ~2.1 MPa), a lower strength (ultimate stress ~75 MPa), a larger extensibility (ultimate strain ~1.2), and a lower energy absorption ability (fracture work ~12 MJ/m^3). The Young's modulus and tensile strength of the spiral silks in the outer region are ~20.8 MPa and ~450 MPa, which are approximately 9.9 and 6.0 times higher than those in the inner. The extensibility of the silks in the outer region is relatively low (with the ultimate strain ~0.7), but its energy absorption capability (fracture work) reaches up to ~77 MJ/m^3, which is ~6.4 times higher than those in the inner. Therefore, the spiral silks near the periphery are stiffer and stronger than the paracentral ones.

TABLE I. Statistics of the mechanical properties of the radial silks in the inner, middle, and outer regions.

	Inner	Middle	Outer
Diameter (μm)	12.1 ± 3.3	11.5 ± 3.9	11.5 ± 3.1
Ultimate strain	0.42 ± 0.13	0.46 ± 0.10	0.46 ± 0.11
Tensile strength (MPa)	539 ± 303	647 ± 339	642 ± 426
Ultimate force (mN)	55.2 ± 16.3	57.6 ± 20.2	56.7 ± 20.3
Young's modulus (GPa)	1.68 ± 2.04	1.23 ± 1.67	1.45 ± 1.91
Fracture work (MJ/m^3)	108 ± 93	123 ± 69	125 ± 98

In contrast to the significant gradient functional variations in the spiral silks along the radial direction of the web, the variations in the mechanical properties of the radial silks are almost negligible, as shown in Fig. 3(b) and Table I. Their tensile strength is ~600 MPa, Young's modulus ~1.5 GPa, and fracture work ~120 MJ/m^3, which are significantly higher than those of all spiral silks. The average strength and Young's modulus of the radial silks are 1.3 and 72.1 times higher than those of the spiral silks in the outer region and 8.0 and 714.3 times higher than those of the spiral

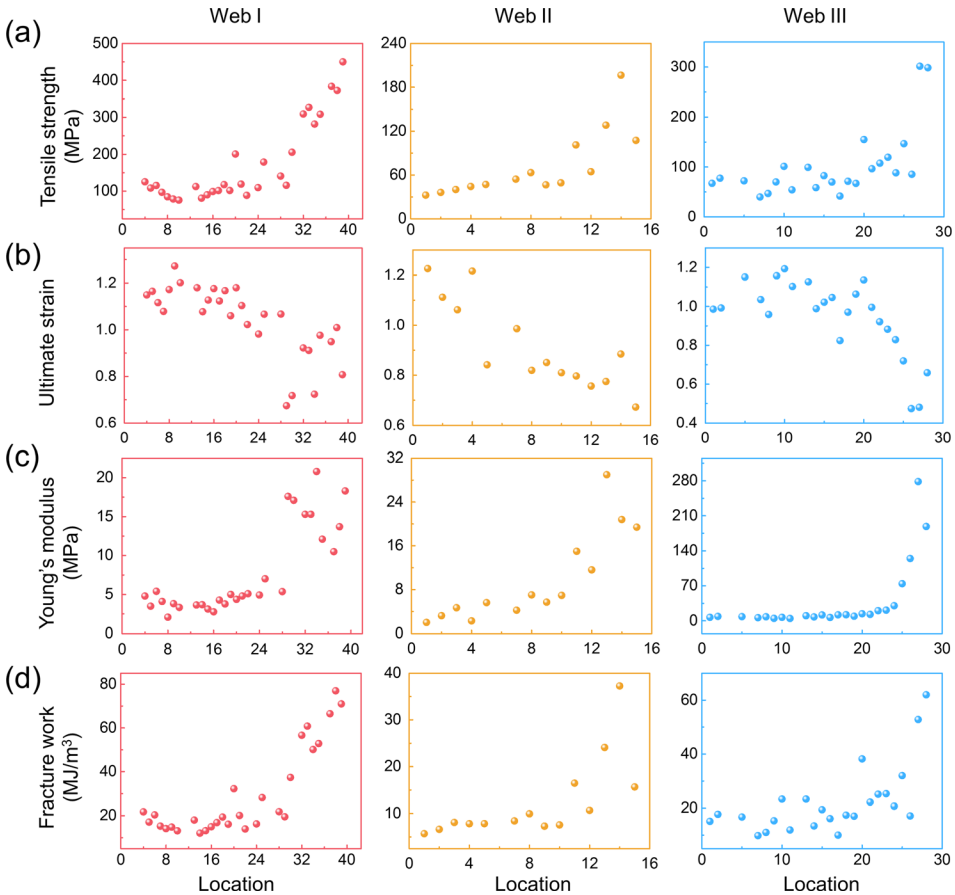

FIG. 4. Gradient variations in the mechanical properties of the spiral silks along the radial direction of the orb web: (a) tensile strength, (b) ultimate strain, (c) Young's modulus, and (d) fracture work, where the location is denoted as the number of spiral silks from the web's center.

silks in the inner region. The energy absorption capability of the radial silks also overmatches that of the spiral silks, amounting to 10.0 and 1.6 times larger than those of the spiral silks in the inner and outer regions, respectively. In the subsequent numerical simulations, therefore, we will assume that the radial silks have uniform mechanical properties.

Using the model in Fig. 2(a), we now perform finite element simulations to examine the effect of the gradient variations in the mechanical properties of the spiral silks on the energy absorption of an orb web. The spiral silks are simplified as concentric circles, instead of an Archimedean spiral curve.[12,30,36] Assume that both radial and spiral silks are linear elastic. Following our experimental measurements, the Young's modulus of the radial silks is fixed as $E_r = 1.0$ GPa. We compare four webs with different Young's modulus E_s for the spiral silks. In the first three examples, we take (i) $E_s = 5.0$ MPa, (ii) $E_s = 25.0$ MPa, and (iii) $E_s = 50.0$ MPa, while in the last example, E_s increases linearly from 5.0 MPa in the innermost layer to 50.0 MPa in the outermost layer.

When an orb web is subjected to the normal impact of a prey, its silk will be stretched due to the out-of-plane deflection of the web.[24] The web absorbs the kinetic energy of the prey, leading to an increase in the total elastic strain energy in the web. In this work, the energy absorption U_{web} is calculated by the increment in the total elastic strain energy in the web from the initial but pre-stretched state to its peak value upon impact. In the calculations, we assume that a concentrated force F is exerted at the mid-point of a spiral silk thread in a sector of the web.

To examine the functional gradient effect, Fig. 5 shows the energy absorptions of the whole web (U_{web}) and the loaded spiral silk (U_{silk}) under different conditions. It can be seen that the total energy absorption of a web depends on both the mechanical properties of the silks and the impact locations. The softer the spiral silk, the larger the energy absorption. The absorbed energy increases as the impact locations move along the radial direction of the web. In the case (i) where $E_s = 5.0$ MPa, for example, the energy absorptions U_{web} change from 0.17 μJ to 0.66 μJ when the position of the impact load ($F = 50\,\mu$N) is moved from the innermost spiral silk to the outermost. For spiral silks with gradient properties, the lowest energy absorption ($U_{web} = 0.17\,\mu$J) occurs when the innermost spiral silk is impacted, while the largest value ($U_{web} = 0.29\,\mu$J) occurs when the force is applied at the 8th spiral silk.

To more clearly illustrate the changing tendency of energy absorption when the impact load is exerted at different positions, Fig. 5(b) shows the energy absorption normalized by that when the force is applied at the innermost silk, $U_{web}/U_{web}^{(1)}$. The ratio between the maximal and the minimal energy absorptions of the gradient web (Case iv) is smaller than 1.65, but the corresponding values of the uniform webs (Cases i–iii) are 3.88, 2.43, and 1.93, respectively. This demonstrates that the functional gradient web has a relatively uniform energy absorption ability regardless of the impact position.

The spiral silk on which the external load directly acts stores a large amount of energy and is most susceptible to damage.[37] Figures 5(c) and 5(d) show the normalized energy U_{silk} stored in the loaded spiral silk. In the web comprising functional gradient spiral silk (Case iv), U_{silk} is substantially smaller than that in a web with a uniform stiffness of spiral silk (Cases i–iii). In Case (iv), the energies U_{silk} change from 0.056 μJ to 0.168 μJ when the position of the impact load is moved from the innermost spiral silk to the outermost, with the largest ratio of variation in energy absorption reaching a factor of 3.0. By contrast, for Cases (i)–(iii), the corresponding U_{silk} values are from 0.055 μJ to 0.61 μJ (a ratio of 11.1 times) in Case (i), 0.015 μJ to 0.238 μJ (a ratio of 15.9 times) in Case (ii), and 0.009 μJ to 0.159 μJ (a ratio of 17.7 times) in Case (iii). This result shows that the functional gradient web has a much better ability to prevent silk breakage due to prey impact and thus is much safer than the uniform webs.

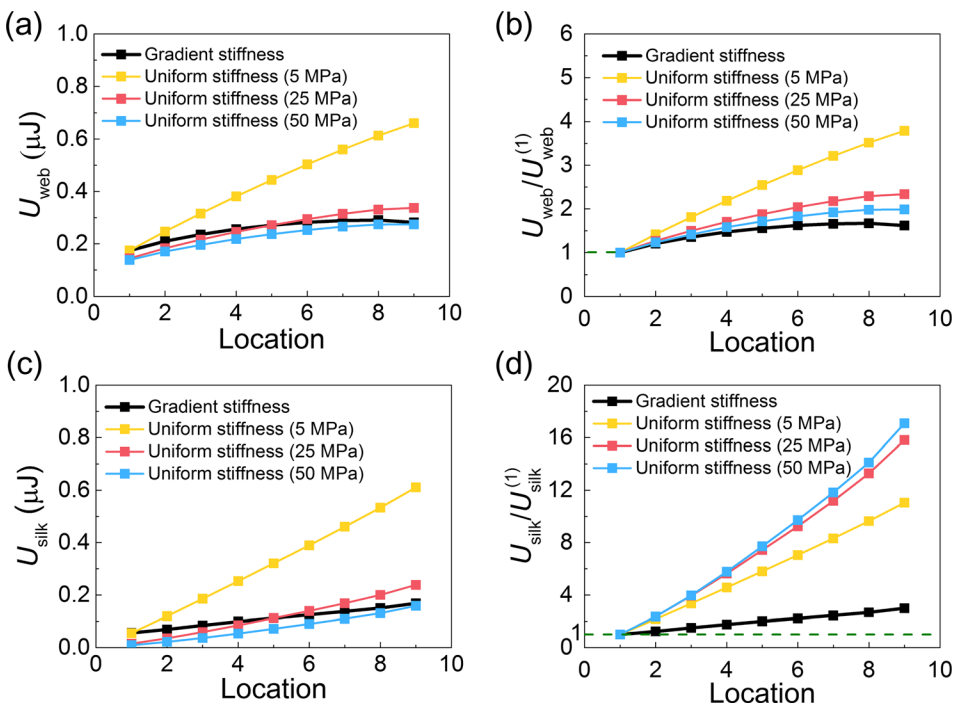

FIG. 5. Numerical results for the energy absorption U_{web} in the whole web and U_{silk} in the impacted silk. (a) Energy absorption U_{web} in the whole web and (b) its normalized value $U_{web}/U_{web}^{(1)}$, where $U_{web}^{(1)}$ is the energy absorption when the prey impacts the middle position of the innermost silk. (c) Energy absorption U_{silk} in the loaded spiral silk and (d) its normalized value $U_{silk}/U_{silk}^{(1)}$, where $U_{silk}^{(1)}$ is the energy absorption when the prey impacts the middle position of the innermost silk. Here, we fix $E_r = 1.0$ GPa.

The above analysis demonstrates that the gradient variation in the mechanical properties of spiral silks can not only enhance the total energy absorption U_{web} of the web but also homogenize the energy storage U_{silk} in the impacted silk. By this mechanism, the orb web exhibits a nearly uniform energy absorption ability regardless of the position where a flying prey impacts the web, and an enhanced structural integrity in preventing silk breakage due to prey impacts.

A spider can weave several types of silks. Among them, the radial silk and the spiral silk have greatly different mechanical properties.[6] The radial silk, composed of major ampullate silk, is crucial for supporting the web frame, whereas the sticky spiral silk, generated by the flagelliform gland, is more compliant and flexible than the radial silk.[6] The spiral and radial silks work synergistically to absorb the kinetic energy when a flying insect is trapped.[7]

Previous studies[24,38] focused on the interspecific or intraspecific difference of the webs,[14,39] while the difference among the silks at different positions in the same web has not been reported. Our experiments indicate an enhancing mechanism in spider web, which arises from the gradient variation in the mechanical properties of the sticky spiral silks along the radial direction of the web. This may be a primary reason that the mechanical parameters reported in the literature have a great scattering. Through the measurement of the silks in 20 sector regions from 10 orb webs weaved by *Araneus ventricosus*, we found that the gradient variations in the mechanical properties of spiral silks are significant and well repeatable, regardless of the spider weight, web dimension, sector location, and silk thread thickness. It is worth emphasizing that though the spiral silks in the outer regions in the web are stiffer and stronger than those in the inner, they are still much softer than the radial silks.

In summary, we have reported a physical mechanism that enhances the energy absorption ability of spider webs, which is attributed to the distinct spatial gradient variations in the mechanical properties of spiral silks. The functional gradient effect can significantly enhance the energy absorption and structural integrity of the web. The results not only help understand the optimal energetic mechanisms of spider webs, but can also provide useful guidelines for designing anti-impact structures.

Support from the National Natural Science Foundation of China (Grant No. 11432008) is acknowledged.

[1]B. L. Karihaloo, K. Zhang, and J. Wang, J. R. Soc., Interface **10**(86), 20130299 (2013).
[2]H. P. Zhao, X. Q. Feng, S. W. Yu, W. Z. Cui, and F. Z. Zou, Polymer **46**(21), 9192 (2005).
[3]Y. Shao, H. P. Zhao, X. Q. Feng, and H. Gao, J. Mech. Phys. Solids **60**(8), 1400 (2012).
[4]J. Aizenberg, J. C. Weaver, M. S. Thanawala, V. C. Sundar, D. E. Morse, and P. Fratzl, Science **309**(5732), 275 (2005).
[5]B. W. Li, H. P. Zhao, and X. Q. Feng, Mater. Sci. Eng. C **31**(2), 179 (2011).
[6]F. G. Omenetto and D. L. Kaplan, Science **329**(5991), 528 (2010).
[7]A. T. Sensenig, K. A. Lorentz, S. P. Kelly, and T. A. Blackledge, J. R. Soc., Interface **9**(73), 1880 (2012).
[8]T. A. Blackledge, N. Scharff, J. A. Coddington, T. Szuts, J. W. Wenzel, C. Y. Hayashi, and I. Agnarsson, Proc. Natl. Acad. Sci. U. S. A. **106**(13), 5229 (2009).
[9]A. T. Sensenig, S. P. Kelly, K. A. Lorentz, B. Lesher, and T. A. Blackledge, J. Exp. Biol. **216**(18), 3388 (2013).
[10]C. P. Liao, K. J. Chi, and I. M. Tso, Behav. Ecol. **20**(6), 1194 (2009).
[11]Y. Zheng, H. Bai, Z. Huang, X. Tian, F. Q. Nie, Y. Zhao, J. Zhai, and L. Jiang, Nature **463**(7281), 640 (2010).
[12]Y. Aoyanagi and K. Okumura, Phys. Rev. Lett. **104**(3), 038102 (2010).
[13]S. W. Cranford, A. Tarakanova, N. M. Pugno, and M. J. Buehler, Nature **482**(7383), 72 (2012).
[14]A. Sensenig, I. Agnarsson, and T. A. Blackledge, J. Evol. Biol. **23**(9), 1839 (2010).
[15]T. Hesselberg and F. Vollrath, J. Exp. Biol. **215**(19), 3362 (2012).
[16]F. Vollrath and D. Porter, Soft Matter **2**(5), 377 (2006).
[17]F. Vollrath, D. Porter, and C. Holland, Soft Matter **7**(20), 9595 (2011).
[18]M. Elices, J. Perez-Rigueiro, G. R. Plaza, and G. V. Guinea, JOM **57**(2), 60 (2005).
[19]F. Vollrath, M. Downes, and S. Krackow, Physiol. Behav. **62**(4), 735 (1997).
[20]A. Walter and M. A. Elgar, Behav. Ecol. Sociobiol. **65**(10), 1909 (2011).
[21]T. Watanabe, Proc. R. Soc. London, Ser. B **267**(1443), 565 (2000).
[22]B. Mortimer, S. D. Gordon, C. Holland, C. R. Siviour, F. Vollrath, and J. F. Windmill, Adv. Mater. **26**(30), 5179 (2014).
[23]A. M. Harmer, P. D. Clausen, S. Wroe, and J. S. Madin, Sci. Rep. **5**, 14121 (2015).
[24]A. Tarakanova and M. J. Buehler, J. R. Soc., Interface **9**(77), 3240 (2012).
[25]Y. Guo, Z. Chang, H. Y. Guo, W. Fang, Q. Li, H. P. Zhao, X. Q. Feng, and H. Gao, J. R. Soc., Interface **15**(140), 20170894 (2018).
[26]L. Eisoldt, A. Smith, and T. Scheibel, Mater. Today **14**(3), 80 (2011).
[27]B. D. Opell and J. E. Bond, Biol. J. Linn. Soc. **70**(1), 107 (2000).
[28]G. V. Guinea, M. Cerdeira, G. R. Plaza, M. Elices, and J. Perez-Rigueiro, Biomacromolecules **11**(5), 1174 (2010).
[29]A. T. Sensenig, I. Agnarsson, and T. A. Blackledge, J. Zool. **285**(1), 28 (2011).
[30]M. S. Alam, M. A. Wahab, and C. H. Jenkins, Mech. Mater. **39**(2), 145 (2007).
[31]A. Soler and R. Zaera, Sci. Rep. **6**, 31265 (2016).
[32]E. Wirth and F. G. Barth, J. Comp. Physiol., A **171**(3), 359 (1992).
[33]R. Zaera, A. Soler, and J. Teus, J. R. Soc., Interface **11**(98), 20140484 (2014).
[34]B. Mortimer, A. Soler, C. R. Siviour, R. Zaera, and F. Vollrath, J. R. Soc., Interface **13**(122), 20160341 (2016).
[35]B. D. Opell and M. L. Hendricks, J. Exp. Biol. **212**(18), 3026 (2009).
[36]H. Yu, J. L. Yang, and Y. X. Sun, J. Bionic Eng. **12**(3), 453 (2015).
[37]Z. Qin, B. G. Compton, J. A. Lewis, and M. J. Buehler, Nat. Commun. **6**, 7038 (2015).
[38]B. O. Swanson, T. A. Blackledge, and C. Y. Hayashi, J. Exp. Zool., Part A **307**(11), 654 (2007).
[39]K. Nakata and S. Zschokke, Proc. R. Soc. London, Ser. B **277**(1696), 3019 (2010).